pH Dependence of Heme Iron Coordination, Hydrogen Peroxide Reactivity, and Cyanide Binding in Cytochrome *c* Peroxidase(H52K)†

Miriam C. Foshay,‡ Lidia B. Vitello, and James E. Erman*

Department of Chemistry and Biochemistry, Northern Illinois University, DeKalb, Illinois 60115

Received December 13, 2003; Revised Manuscript Received February 3, 2004

ABSTRACT: Replacement of the distal histidine, His-52, in cytochrome *c* peroxidase (CcP) with a lysine residue produces a mutant cytochrome *c* peroxidase, CcP(H52K), with spectral and kinetic properties significantly altered compared to those of the wild-type enzyme. Three spectroscopically distinct forms of the enzyme are observed between pH 4.0 and 8.0 with two additional forms, thought to be partially denatured forms, making contributions to the observed spectra at the pH extremes. CcP(H52K) exists in at least three, slowly interconverting conformational states over most of the pH range that was investigated. The side chain ϵ-amino group of Lys-52 has an apparent pK_a of 6.4 ± 0.2, and the protonation state of Lys-52 affects the spectral properties of the enzyme and the reactions with both hydrogen peroxide and HCN. In its unprotonated form, Lys-52 acts as a base catalyst facilitating the reactions of both hydrogen peroxide and HCN with CcP(H52K). The major form of CcP(H52K) reacts with hydrogen peroxide with a rate ∼50 times slower than that of wild-type CcP but reacts with HCN ∼3 times faster than does the wild-type enzyme. The major form of the mutant enzyme has a higher affinity for HCN than does native CcP.

Cytochrome *c* peroxidase (CcP),[1] a heme protein found in *Saccharomyces cerevisiae*, belongs to a superfamily of peroxidases and catalase-peroxidases, all of which have a similar structure in the distal heme pocket. Class I includes CcP, the ascorbate peroxidases of higher plants and green algae, and the catalase-peroxidases which are found in bacteria and lower eukaryotes. Of 12 ascorbate peroxidases and 15 catalase-peroxidases that have been investigated, all but one have the same catalytic triad, Arg-x-x-Trp-His (*1*). Once the structure of CcP was determined (*2*, *3***)**, the configuration of the three conserved residues in the distal pocket provided insight into the probable reaction mechanism. The location of the conserved histidine in CcP, His-52, is directly above the heme iron, leading Poulos and Kraut to postulate that His-52 acts as an acid−base catalyst in the reduction of hydrogen peroxide (*4*). According to this scheme, His-52 serves two roles. As a base catalyst, it extracts a proton from the incoming H_2O_2, and as an acid catalyst, it donates the proton to the leaving H_2O. The charged imidazolium side chain contributes to destabilization and heterolytic cleavage of the oxygen−oxygen bond in the bound peroxide.

Evidence to support this model comes from several sources. Replacement of His-52 with leucine decreases the reaction rate by more than 5 orders of magnitude, providing support for the role of His-52 as a base catalyst (*5*). X-ray crystallography shows N_ϵ of His-52 to be within hydrogen bonding distance of the distal oxygen of a model CcP Fe(II)−O_2 complex (*6*), and the imidazole side chain of His-52 is held in an optimal catalytic position by hydrogen bonding between N_δ of His-52 and the amide oxygen of Asn-82 (*7*). The pH dependence of the reaction between hydrogen peroxide and CcP also provides evidence for base catalysis, with the enzyme becoming optimally active above pH 5.5 in nitrate-containing buffers (*8*) and above pH 3.9 in phosphate-containing buffers (*9*). The inflections in the activity−pH profiles have been assigned to the pK_a values for His-52 in these two buffer systems.

If His-52 serves as an acid−base catalyst, then other bases should to be able to serve this role. Arginine and lysine are stronger bases than histidine and are normally protonated over the pH range of 4−8. However, the environment of the distal heme pocket in CcP substantially lowers the pK_a of His-52, and if this were to occur for a lysine residue in the same position, the effect of base strength on the hydrogen peroxide reactivity could be investigated. Steric considerations may also affect the ability of Lys-52 to act as a base catalyst. The lysine side chain is more flexible than the imidazole side chain of His-52, and the ϵ-amino group may take up different conformations within the heme pocket, not all of which would be optimal for catalytic activity.

CcP reacts preferentially with ligands that diffuse into the binding site as a neutral species, dissociate a proton, and bind to the ferric heme iron as the anion (*9*−*11*). HCN is a good ligand to use as a surrogate for hydrogen peroxide, since it exists in the neutral form between pH 4 and 8 where CcP is stable and its binding to the heme iron can be

† This work was supported in part by grants from the National Science Foundation (MCB-9513047) and the National Institutes of Health (R15 GM59740).

* To whom correspondence should be addressed. Phone: (815) 753-1181. Fax: (815) 753-4802. E-mail: jerman@niu.edu.

‡ Current address: Department of Biochemistry and Molecular Genetics, University of Illinois at Chicago, Chicago, IL 60612.

[1] Abbreviations: CcP, cytochrome *c* peroxidase; CcP(H52K), cytochrome *c* peroxidase in which His-52 has been replaced with a lysine residue; SVD, singular-value decomposition.

10.1021/bi036240j CCC: $27.50
Published on Web 04/07/2004

facilitated by base catalysis of a group at position 52. Unlike hydrogen peroxide, cyanide does not oxidize the protein, and the binding of cyanide can be monitored kinetically as well as under equilibrium conditions, providing association and dissociation rate constants and equilibrium constants for characterizing the reaction.

In this study, the absorption spectrum of CcP(H52K) and the reactions with hydrogen peroxide and HCN were investigated between pH 4 and 8. Comparison of the properties of CcP(H52K) with those of wild-type CcP provides useful insights into the reaction mechanism and the alterations induced by lysine substitution at position 52.

MATERIALS AND METHODS

Starting Clones and Mutagenesis. J. Satterlee (Washington State University, Pullman, WA) kindly provided the expression system for the recombinant CcP used in this study (*12*). The cloned CcP gene was modified so that the amino acid sequence of the expressed protein is identical to that of baker's yeast CcP (*13*). In particular, the cloned protein has Thr-53 and Asp-152. The CcP gene is inserted into the multiple cloning site of Novagene vector pET24a(+) under the control of the T7 promoter. Recombinant CcP was expressed in *Escherichia coli* strain BL21(DE3) using a modification of the rapid isolation technique published by Teske *et al*. (*14*). The N-terminal methionine required for initiation of protein synthesis is removed from the recombinant CcP produced by this expression system so that there are no N-terminal modifications in the recombinant CcP compared to baker's yeast CcP (*14*). CcP(H52K) was created using Stratagene Quik-Change mutagenesis and sequenced from 5′ to 3′ and from 3′ to 5′ to ensure that, except for the intended mutation, the protein was identical to the published sequence.

Buffer Preparation. Between pH 4.0 and 5.0, buffers contained 0.010 M total acetate and sufficient potassium phosphate to bring the ionic strength to 0.10 M. Between pH 5.5 and 8.0, 0.10 M ionic strength phosphate buffers were used; the ionic strength was kept constant by allowing the total phosphate concentration to vary with pH. Salts and acetic acid were reagent-grade. Water was deionized by reverse osmosis and ion exchange chromatography. Buffers were stored at room temperature in capped containers and used within 5 working days.

Protein Concentration Determination. The extinction coefficient for CcP(H52K) was determined using the pyridine hemochromogen method of Berry and Trumpower (*15*) under the assumption that the apoprotein and heme bound with 1:1 stoichiometry. There is no evidence that CcP(H52K) samples contain the apoprotein, but small amounts of the apoprotein will not affect the results of these studies. The extinction coefficient of the heme group in CcP(H52K) is 87 mM^{-1} cm^{-1} at the Soret maximum in 0.10 M ionic strength phosphate buffer (pH 6.0) and was used to determine the concentration of CcP(H52K).

Time and pH Dependence of the CcP(H52K) Spectra. The spectrum of CcP(H52K) changes slowly after a pH perturbation, and the time dependence of the spectral changes was investigated using either a Cary 3E UV−vis spectrophotometer or a Hewlett-Packard 8452A diode-array spectrophotometer (2 nm resolution). Crystalline CcP(H52K) was dissolved in 0.10 M ionic strength potassium phosphate/acetate buffer (pH 4.0) at a concentration of 600−750 μM. Aliquots of the concentrated enzyme were diluted to ~5 μM with an appropriate buffer and incubated for various lengths of time prior to determining the absorption spectrum. Spectra were determined at every 0.5 pH unit between pH 4 and 8, and the incubation time interval varied between 1 min and 24 h. Global analysis of the time and pH dependence of the spectra of CcP(H52K) was carried out using singular-value decomposition (SVD) and nonlinear regression analysis with the aid of SPECFIT/32 (Spectrum Software Associates).

Hydrogen Peroxide Concentration. Reagent-grade hydrogen peroxide (30%, v/v) was purchased from Aldrich Chemical Co. The concentration of hydrogen peroxide stock solutions was determined in two ways: by titration with cerium sulfate (*16*) and from the absorbance at 240 nm using an extinction coefficient of 39.4 M^{-1} cm^{-1} (*17*).

Kinetics of Compound I Formation. Formation of Compound I was studied under pseudo-first-order conditions, with peroxide concentrations being 10−100-fold greater than the CcP concentration. CcP(H52K) concentrations were 1−2 μM. Stopped-flow experiments were performed with an Applied Photophysics DX.17MV stopped-flow spectrophotometer at 25 °C and a standard wavelength of 424 nm. At least nine traces were collected at each hydrogen peroxide concentration. Data analysis was performed using the SpectraKinetic Workstation provided by Applied Photophysics, Ltd., and SigmaPlot (SPSS, Inc.). The observed rate constants (k^{obs}) were plotted as a function of the hydrogen peroxide concentration, and the slope of the plot gave the apparent bimolecular rate constant (k^{app}).

Cyanide Binding. The rate of cyanide binding at 25 °C was measured under pseudo-first-order conditions ([HCN] > 50 μM and [CcP(H52K)] ~ 2 μM) by observing the reaction at 428 nm with the Applied Photophysics stopped-flow spectrophotometer. The observed rate constants were fit to eq 1

$$k^{obs} = k_a[KCN] + k_d \quad (1)$$

where k_a is the rate of cyanide binding and k_d is the rate of dissociation. Equilibrium constants for cyanide binding were determined spectrophotometrically at pH 4, 6, and 8. Aliquots of HCN were added to ~5 μM CcP(H52K). The absorbance at 428 nm was monitored as a function of time after each HCN addition and recorded after the reading stabilized. Data analysis was performed using SigmaPlot.

RESULTS AND DISCUSSION

pH Dependence of the Spectrum. The spectrum of native CcP(H52K) at pH 4, 6, and 8 is shown in Figure 1. The spectrum of CcP(H52K) is significantly more pH-dependent in this region than that of wild-type CcP (*18*, *19*). At pH 4.0, the spectrum of CcP(H52K) is indicative of a five-coordinate, high-spin heme group, with a Soret maximum at 406 nm, slightly blue-shifted compared to the wild-type CcP Soret maximum at 408 nm. At pH 6.0, the Soret band shifts to 407 nm and is still predominantly five-coordinate and high-spin. At pH 8.0, the mutant enzyme contains a six-coordinate, low-spin species as can be seen by the red shift in the Soret maximum to 411 nm and the decrease in the shoulder at 380 nm. The magnitudes of the prominent charge-

Table 1: Spectroscopic Properties of CcP(H52K) and Derivatives[a]

species	pH	$\delta\ \lambda\ (\epsilon)$	Soret $\lambda\ (\epsilon)$	CT2 $\lambda\ (\epsilon)$	$\beta\ \lambda\ (\epsilon)$	$\alpha\ \lambda\ (\epsilon)$	CT1 $\lambda\ (\epsilon)$
CcP(H52K)	4.0	~380sh (68.4)	406 (90.2)	506 (10.3)	~544sh (7.8)	~584sh (3.4)	638 (3.5)
CcP(H52K)	6.0	~380sh (68.5)	407 (87.5)	512 (10.7)	~536sh (10.1)	~584sh (4.3)	647 (3.1)
CcP(H52K)	8.0	~360sh (40.7)	411 (80.4)		535 (9.1)	~576sh (6.2)	~620sh (3.5)
A (SVD)[b]		~376sh (72.7)	396 (77.2)	500 (7.3)	~544sh (5.2)	-	624 (2.9)
B (SVD)		~380sh (66.8)	408 (101)	506 (11.1)	~544sh (8.5)	~584sh (3.6)	640 (3.7)
C (SVD)		~380sh (70.8)	401 (78.9)	511 (10.5)	535 (10.2)	~584sh (4.3)	651 (3.0)
D (SVD)			412 (95.4)	506 (9.6)	537 (10.3)	~584sh (5.5)	~643sh (2.6)
E (SVD)		~360sh (41.5)	410 (68.5)	~487sh (7.4)	533 (8.0)	562 (7.1)	~615sh (4.4)
CcP(H52K) Compound I	6.0	348 (29.8)	420 (102.2)		530 (13.2)	560 (15.2)	
CcP(H52K)−CN	6.0	362 (32.2)	424 (98.6)		540 (12.1)	~582sh (7.5)	

[a] Band maxima (λ) are given in nanometers, and extinction coefficients (ϵ) are given in units of $mM^{-1}\ cm^{-1}$. Positions of bands that appear as shoulders (sh) are only approximate. Species A−E are defined in eq 2 of the text. [b] Spectral properties of species A when pK_{E1} is 3.4.

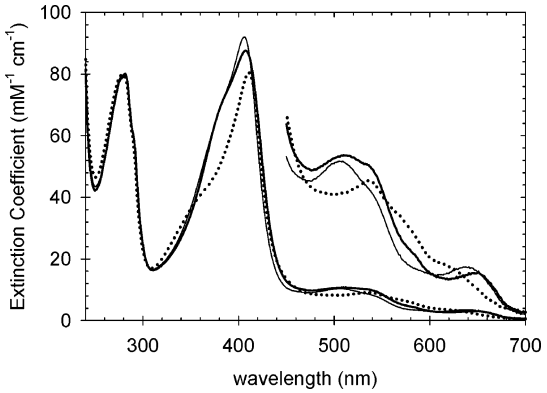

FIGURE 1: Spectra of native CcP(H52K) at pH 4, 6, and 8. Experimental spectra acquired 1 min after dilution from a pH 4 stock solution into appropriate buffers. The visible regions of the spectra are expanded 5-fold on the vertical scale: thin solid line for pH 4.0, thick solid line for pH 6.0, and dotted line for pH 8.0. Experimental conditions: 5 μM CcP(H52K) and 25 °C.

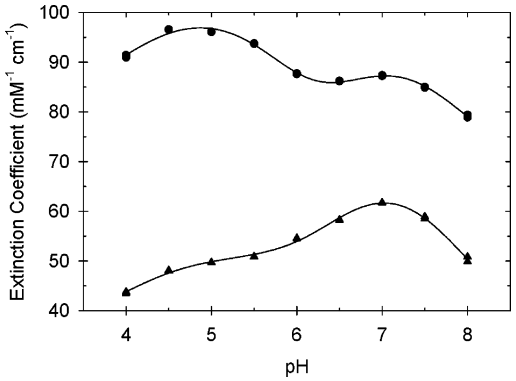

FIGURE 2: pH dependence of the extinction coefficients for CcP(H52K) at 408 (●) and 424 nm (▲). Four pH-dependent transitions are apparent. The solid lines were calculated for the mechanism shown in eq 2 and using the pK values given in Table 2.

transfer bands apparent at pH 4 are diminished at pH 8 and replaced by α and β bands near 535 and 576 nm, respectively, indicating a shift from a high-spin to a low-spin configuration. The wavelengths and extinction coefficients of prominent bands at pH 4, 6, and 8 are given in Table 1.

The spectrum of CcP(H52K) is both time- and pH-dependent. If enzyme, prepared at one pH, is diluted into buffer of another pH, it takes several minutes to an hour before the spectrum stabilizes. The initial pH-induced changes are reversible between pH 4 and 8, and the time-dependent changes are small compared to the pH-induced changes. In this study, spectra were collected 1 min and 1 h after enzyme was diluted into each buffer. The spectrum of CcP(H52K) was determined at intervals of 0.5 pH unit, and a plot of the absorbance at 408 and 424 nm 1 min after dilution into an appropriate buffer is shown in Figure 2. The data in Figure 2 suggest a minimum of four pH-induced transitions are affecting the spectrum of CcP(H52K) between pH 4 and 8. The data at 408 nm clearly show three transitions, one occurring below pH 4.5, one occurring between pH 4.5 and 6, and a third occurring above pH 7. The fourth transition occurs between pH 6 and 7 and is best seen at 424 nm.

Global analysis of the pH dependence of the spectra of CcP(H52K) was carried out using singular-value decomposition (SVD) (*20*) and nonlinear regression analysis. SVD of the pH-dependent spectra gives six eigenvectors with eigenvalues larger than the noise level. However, the smallest eigenvalue is less than a factor of 2 above the noise level.

Table 2: pK_E Values for Interconversion of CcP(H52K) Species Determined by SVD Analysis[a]

transition	calcd value (1 min)	calcd value (1 h)
pK_{E1}[b]	3.4−4.0	3.4−4.0
pK_{E2}	5.9 ± 0.2	5.7 ± 0.2
pK_{E3}	6.5 ± 0.2	6.6 ± 0.2
pK_{E4}	7.9 ± 0.2	7.8 ± 0.2

[a] A stock solution of enzyme was diluted into different pH buffers, and spectra were recorded after 1 min and 1 h. [b] Reasonable results were obtained with pK_{E1} values between 3.4 and 4.0.

Additional analyses indicate that the eigenvector with the smallest eigenvalue contains little spectral information. The data were fit to a model containing five spectroscopically distinct species related by four acid dissociations (eq 2).

$$A \overset{pK_{E1}}{\rightleftharpoons} B \overset{pK_{E2}}{\rightleftharpoons} C \overset{pK_{E3}}{\rightleftharpoons} D \overset{pK_{E4}}{\rightleftharpoons} E \qquad (2)$$

The value of pK_{E1} could not be determined since a low-pH limit of absorbance was not determined (Figure 2). Analysis was carried out by fixing the value of pK_{E1} and allowing the other dissociation constants to vary. Reasonable spectra for species A were obtained with pK_{E1} values between 3.4 and 4.0. The value of pK_{E1} had little effect on the spectra of species B−E and on the other pK_E values, so we decided to fix pK_{E1} at the lower limit of 3.4 in the final analysis. The results of the SVD and nonlinear regression analysis provide spectra for the five enzyme species (Table 1) and best-fit values for the acid dissociation constants (Table 2). The calculated spectra for species A−E are identical whether the enzyme is incubated for 1 min or 1 h. Values of pK_E vary

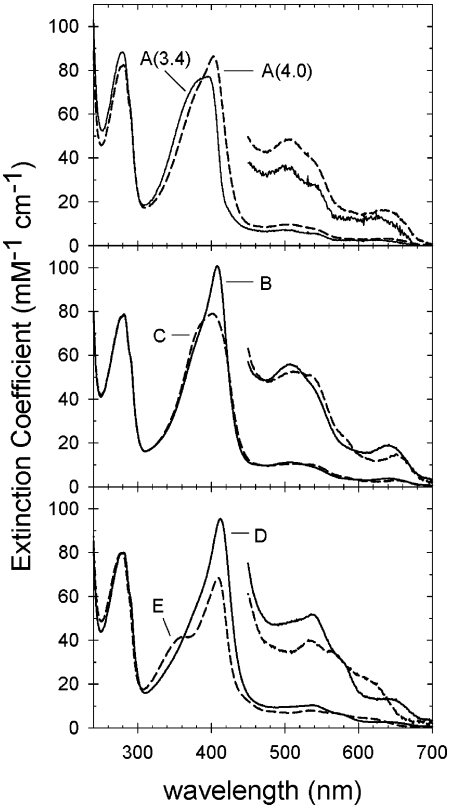

FIGURE 3: Calculated spectra of CcP(H52K) species A−E. Species are defined in eq 2 of the text, and spectra were calculated using singular-value decomposition and nonlinear regression analysis of the pH dependence of the spectrum of CcP(H52K) between pH 4 and 8. In each panel, the visible regions of the spectra are expanded 5-fold on the vertical scale. In the top panel, solid and dashed lines represent species A calculated when pK_{E1} is equal to 3.4 and 4.0, respectively. In the middle panel, species B is represented by a solid line and species C by a dashed line. In the bottom panel, species D is represented by a solid line and species E by a dashed line.

by 0.1−0.2 unit over the 1 h incubation period (Table 2). The time dependence of the spectrum of CcP(H52K) appears to be due to a slight stabilization of species C and E relative to species B and D.

Calculated spectra for species A−E are shown in Figure 3. The calculated spectrum of species A is critically dependent upon the value of pK_{E1} (Figure 3). If pK_{E1} is set to its upper limit of 4, the calculated spectrum of species A indicates a five-coordinate, high-spin heme group similar to that of wild-type CcP but with slightly diminished extinction coefficients. If pK_{E1} is set to its lower limit of 3.4, the spectrum of species A indicates a denatured form of the enzyme. Since wild-type CcP is rapidly denatured below pH 4 with irreversible loss of >99% of its activity at pH 3 (*21*), the most reasonable interpretation for the decrease in absorption seen below pH 4.5 is that this is the beginning of the spectroscopic changes associated with acid denaturation of CcP(H52K).[2]

The computed spectrum of species B (Table 1 and Figure 3) is almost identical to that of wild-type CcP, indicating that species B contains a five-coordinate, high-spin heme group (*22*). The ionization characterized by a pK_{E2} near 5.8 (eq 2 and Table 2) causes a transition between species B and C. Species C appears to be a mixture of high- and low-spin forms (Figure 3) with charge-transfer bands near 511 and 651 nm and prominent shoulders near 535 and 584 nm characteristic of the α and β bands, respectively (Table 1). The ionizable group associated with the B to C transition is enigmatic. There is evidence that a group with a pK_a near 5 in wild-type yeast CcP influences proton uptake and release during the reaction with hydrogen peroxide and with the binding of fluoride and is required to satisfy microscopic reversibility in fluoride binding (*23*, *24*). There is also an inflection near 4.5 in the pH dependence of the hydrogen peroxide reaction with CcP(H52L) that may be associated with this ionizable group (*5*). Suggestions for the identity of the group have been Asp-235 or one of the two propionates on the porphyrin ring. Conversion of Asp-235 to an asparagine residue has profound consequences on heme coordination in CcP (*22*) such that it has been impossible to determine the pK_a for the side chain carboxylate of Asp-235. Whatever the group, its effect on heme coordination in CcP(H52K) is to convert five-coordinate species B into a mixed spin species with a water most likely coordinated to the heme iron in species C.

On the basis of the pH dependence of the reaction with H_2O_2 (see below), pK_{E3} and the C−D transition (eq 2) are attributed to the deprotonation of the ϵ-amino group of Lys-52. Species D is predominantly low-spin but with a minor high-spin component (Table 1). The low-spin form must be six-coordinate, and there are three possibilities for the sixth ligand: water, hydroxide, or Lys-52. The ϵ-amino group of Lys-52 is a strong field ligand, and if Lys-52 is coordinated to the heme iron in species D, the spectrum should be entirely low-spin rather than a mixture of high- and low-spin. The spectroscopic changes for the C−D transition are the likely result of altered hydrogen bonding in the heme pocket upon deprotonation of Lys-52. The most probable iron ligand in species D is a water molecule that is also hydrogen-bonded to Lys-52.

The lowered absorptivity of species E in the Soret region (Table 1 and Figure 3) suggests partial denaturation and conversion to a six-coordinate, low-spin form. The two possible sixth ligands are hydroxide or the Lys-52 side chain. It has been proposed that His-52 is coordinated to the heme iron in wild-type CcP at high pH (*18*), at elevated temperatures (*25*), and in the Fe(II) form of the enzyme (*26*, *27*). The coordination of His-52 appears to be associated with deprotonation of His-181, which confers increased flexibility to the polypeptide chain allowing His-52 to move toward the heme iron (*27*). Coordination of His-52 to the heme makes it quite likely that Lys-52 can also coordinate. Ligation of Lys-52 to the heme iron in species E is supported by its spectroscopic properties. The positions of the α and β bands (562 and 533 nm, respectively) in species E favor bis-nitrogen coordination to the heme iron. Bis-imidazole complexes have α and β band positions in the ranges of 561−568 and 526−533 nm, respectively, while hydroxide-bound heme proteins have α and β band positions in the ranges of 570−582 and 537−544, respectively (*22*).

Kinetics of Compound I Formation. The reaction between hydrogen peroxide and CcP(H52K) to form CcP(H52K) Compound I is biphasic between pH 4.5 and 7.0 with the

[2] During the initial review of the manuscript, a reviewer suggested that formation of species A could also be associated with binding of acetic acid to CcP(H52K). This remains a possibility.

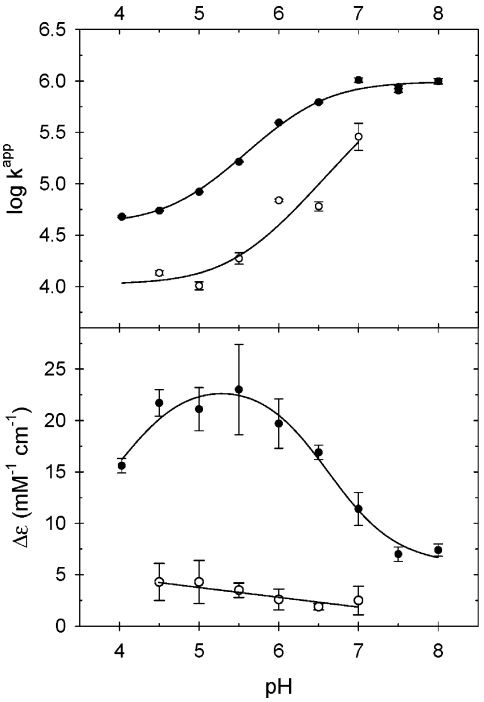

FIGURE 4: (Top) pH dependence of the apparent bimolecular rate constants for the reaction between hydrogen peroxide and CcP(H52K): (●) fast reaction phase and (○) slow reaction phase. (Bottom) Amplitude of the two kinetic phases observed at 424 nm: (●) fast reaction phase and (○) slow reaction phase. Experimental conditions: 1−2 μM CcP(H52K), 10−100 μM H_2O_2, and 25 °C.

fast phase of the reaction ~7 times faster than the slow phase. Both observed rate constants are linear functions of the hydrogen peroxide concentration, and apparent bimolecular rate constants can be determined from the slopes of the observed rate constant versus hydrogen peroxide concentration. The pH dependence of the apparent bimolecular rate constants and the amplitudes of the two reaction phases are shown in Figure 4. The slow phase is only observed between pH 4.5 and 7.0, and its amplitude averages ~15% of the total absorbance change at 424 nm.

The pH dependence of the bimolecular rate constant for the major phase of the hydrogen peroxide reaction can be fit to an equation describing the involvement of a single ionizable group in the enzyme (eq 3).

$$k_1^{app} = \frac{k_{1A}[H^+] + k_{1B}K_E}{[H^+] + K_E} \quad (3)$$

Fitting the data shown in Figure 4 for k_1^{app} to eq 3 gives best-fit values of 6.3 ± 0.1, (4.2 ± 0.8) × 10^4 M^{-1} s^{-1}, and (9.3 ± 1.0) × 10^5 M^{-1} s^{-1} for pK_E, k_{1A}, and k_{1B}, respectively. These results are collected in Table 3. The solid line through the k_1^{app} data in Figure 4 was calculated using eq 3 and the parameters given in Table 3. The rate constant for the minor reaction phase (k_2^{app}) parallels k_1^{app}. The best-fit value for k_{2A} (analogous to k_{1A} in eq 3) equals (1.1 ± 0.2) × 10^4 M^{-1} s^{-1}. Values for pK_E and k_{2B} (analogous to k_{1B}) cannot be determined since a high-pH limit is not established for the minor reaction phase.

The amplitudes of the reaction provide additional information about the hydrogen peroxide−CcP(H52K) reaction. Figure 4 shows that the amplitude of the major reaction phase decreases substantially as the pH increases from pH 5.5 to 7.5. The decrease in amplitude is primarily due to changes in the absorbance of the ferric enzyme. Species D is a low-spin form of the enzyme with a significantly higher absorptivity at 424 nm than species B and C, and the conversion of species D to Compound I results in a smaller change in absorbance compared to oxidizing species B and C to Compound I. Attributing the amplitude change between pH 4.5 and 8.0 to single-proton dissociation gives an apparent pK_a of 6.6 ± 0.2. The pK_a of 6.6 is similar to the pK_a values obtained by fitting the pH dependence of k_1^{app} (6.3 ± 0.1) and the spectral transition from species C to D (6.5 ± 0.2 and 6.6 ± 0.2), suggesting that all three phenomena are influenced by the same ionization in CcP(H52K). We attribute this ionization to the side chain ϵ-amino group of Lys-52 and assign a weighted average value of 6.4 ± 0.2 to pK_{E3}.

Table 3: Kinetic Rate Constants for Formation of CcP(H52K) Compound I[a]

	pK_E^{kin}	k_{iA} (M^{-1} s^{-1})	k_{iB} (M^{-1} s^{-1})
k_1^{app}	6.3 ± 0.1	(4.2 ± 0.8) × 10^4	(9.3 ± 1.0) × 10^5
k_2^{app}	ND[b]	(1.1 ± 0.2) × 10^4	ND[b]

[a] k_1^{app} represents the rate constant for the major phase of the reaction accounting for ~85% of the reaction amplitude observed at 424 nm. [b] Not determined.

At high pH, Lys-52 functions as a base catalyst and the rate of binding of hydrogen peroxide to CcP(H52K) is (9.3 ± 1.0) × 10^5 M^{-1} s^{-1}, only ~50 times slower than the reaction between hydrogen peroxide and wild-type yeast CcP (*8*). Interestingly, protonation of Lys-52 only decreases the rate of the reaction by a factor of 22, to a value of (4.2 ± 0.8) × 10^4 M^{-1} s^{-1}. Even though protonated Lys-52 cannot act as a base catalyst, the rate constant at low pH is ~300 times faster than the rate constant for CcP(H52L), a mutant in which the distal histidine is replaced with a nonpolar group, ~100-fold faster than the reaction of model porphyrins and metmyoglobin with hydrogen peroxide, and approximately the same as the estimated upper limit for the reaction between hydrogen peroxide and wild-type CcP when the distal histidine is protonated (*5*, *28*). This evidence indicates that the acidic forms of CcP(H52K) are highly accessible to hydrogen peroxide and that other factors besides base catalysis by the residue in position 52 may be involved in facilitating the reaction between CcP and hydrogen peroxide.

Stability of CcP(H52K) Compound I. The endogenous decay of CcP(H52K) Compound I back to a ferric form of the enzyme was investigated at pH 4, 6, and 8. At pH 6.0, CcP(H52K) Compound I decays back to the ferric form of the enzyme in a simple first-order process with a half-time of 2.5 h. At pH 6, CcP(H52K) Compound I is almost as stable as Compound I of wild-type CcP (*29*). CcP(H52K) Compound I is significantly less stable at the pH extremes. At pH 4, the decay is biphasic with 59% of the total absorbance change occurring with a half-life of 4.8 min and the remainder of the decay occurring with a half-life of 1.3 h. At pH 8.0, 54% of the absorbance change occurs with a half-life of <10 s and the remainder with a half-life of 1.0 h. The spectra of the decay products indicate enzyme modification during the endogenous reduction of the oxidized sites in CcP(H52K) Compound I (*30*, *31*).

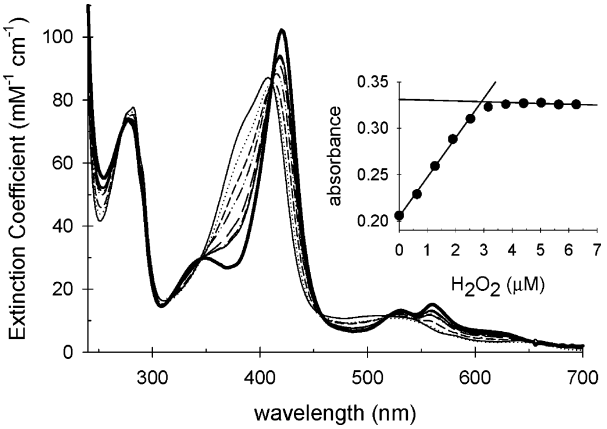

FIGURE 5: Titration of CcP(H52K) with hydrogen peroxide at pH 6 and 25 °C. Spectra of the enzyme were recorded after each addition of hydrogen peroxide. Native CcP(H52K) is represented by a solid thin line. Selected spectra after hydrogen peroxide addition are shown with thin dotted lines, dashed lines, dashed−dotted lines, etc. The thick solid line is a calculated spectrum for 100% conversion of CcP(H52K) to Compound I. The inset is a plot of the absorbance at 424 nm for 3.74 μM enzyme as a function of the amount of added hydrogen peroxide. The equivalence point corresponds to 0.76 mol of hydrogen peroxide reacting per mole of CcP(H52K).

Titration of CcP(H52K) with Hydrogen Peroxide. CcP(H52K) was titrated with hydrogen peroxide to determine the stoichiometry of the reaction. Titrations were performed at every half-pH unit over the pH range of 4.0−8.0. At pH 6.0, CcP(H52K) Compound I is stable enough that multiple aliquots of hydrogen peroxide could be added to the enzyme and the spectrum measured after each addition on a diode-array spectrophotometer. The results of such a titration are shown in Figure 5, where the spectrum of the sample after addition of representative aliquots of H_2O_2 is shown. The inset in Figure 5 shows the absorbance at 424 nm plotted against the concentration of added H_2O_2 with determination of the equivalence point. At pH 6.0, the ratio of hydrogen peroxide added to CcP(H52K) at the equivalence point is 0.76 ± 0.01 (four trials).

CcP(H52K) Compound I decays too rapidly to determine an accurate equivalence point at pH 8, but data can be acquired between pH 4 and 7.5 using an alternative titration procedure in which new enzyme samples are used for each point on the titration curve. The stoichiometric ratio is relatively independent of pH, varying between 0.68 at pH 7.5 and 0.80 at pH 5.5. The average value is 0.75 ± 0.04, indicating that 25% of CcP(H52K) does not react with hydrogen peroxide under the conditions of the titration experiments. The unreactive enzyme could be in conformations that do not equilibrate with the reactive forms on the time scale of the titration experiments or could be misfolded enzyme.

The spectrum of CcP(H52K) Compound I can be estimated from the data shown in Figure 5. If it is assumed that the spectra of the reactive and unreactive forms of the ferric enzyme are identical, the spectrum of CcP(H52K) Compound I can be calculated from the spectrum of the hydrogen peroxide-oxidized enzyme after correcting for the unreactive ferric enzyme. The calculated spectrum is shown by the thick solid line in Figure 5, and spectral properties are collected in Table 1. The calculated spectrum of CcP(H52K) Compound I has absorption maxima at 420, 530, and 560 nm with extinction coefficients of 102, 13.2, and 15.2 mM^{-1} cm^{-1}, respectively. This spectrum is very similar to that of recombinant CcP Compound I, which also has absorption maxima at 420, 530, and 560 nm with extinction coefficients of 107, 12.9, and 14.7 mM^{-1} cm^{-1}, respectively.

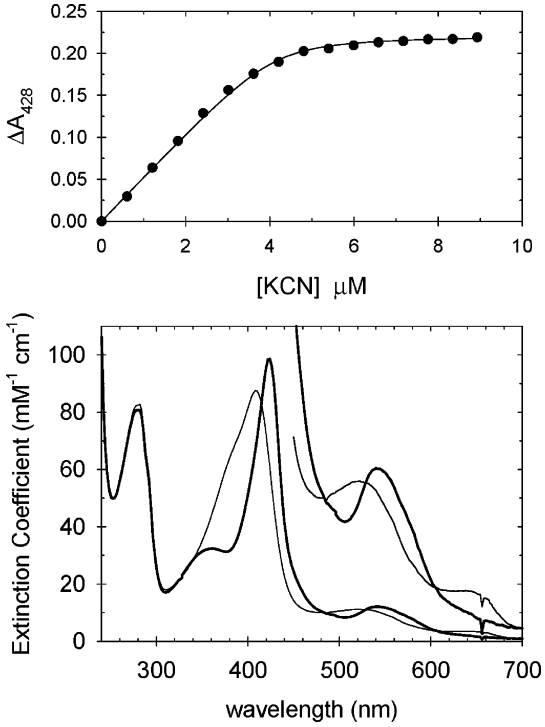

FIGURE 6: Titration of CcP(H52K) with cyanide at pH 6.0 and 25 °C. Bottom panel: thin solid line for the spectrum of CcP(H52K) and thick solid line for the spectrum of the CcP(H52K)−cyanide complex. Band positions and extinction coefficients for the mutant enzyme and its cyanide complex are collected in Table 1. Top panel: (●) absorbance at 428 nm for 4.13 μM CcP(H52K) as a function of the amount of added cyanide and (−) nonlinear regression analysis best-fit line to eq 4 in the text. The best-fit value for K_d is 100 ± 30 nM at pH 6.0. Values for K_d were also determined at pH 4.0 (700 ± 150 nM) and pH 8.0 (55 ± 29 nM).

Binding of Cyanide to CcP(H52K). Figure 6 shows a typical titration of CcP(H52K) with cyanide, monitoring the reaction at 428 nm. The absorbance change was fit to a simple 1:1 binding model where the change in absorbance is given by eq 4.

$$\Delta A = \frac{\Delta A_\infty}{2E_T}[L_0 + E_T + K_D - \sqrt{(L_0 + E_T + K_D)^2 - 4E_T L_0}] \quad (4)$$

where L_0, E_T, K_D, and ΔA_∞ represent the total ligand concentration, the total enzyme concentration, the equilibrium dissociation constant, and the change in absorbance at infinite concentration of ligand, respectively. The binding of cyanide is quite strong with K_D values of 700 ± 150, 100 ± 30, and 55 ± 29 nM at pH 4.0, 6.0, and 8.0, respectively. These values indicate stronger binding of HCN to CcP(H52K) than to wild-type CcP (*12*). The binding is so strong that equivalence points can be determined from the titration curves. More than 95% of the enzyme binds cyanide at all three pH values in distinct contrast to the 75% of the enzyme that reacts with hydrogen peroxide between pH 4.0 and 7.5.

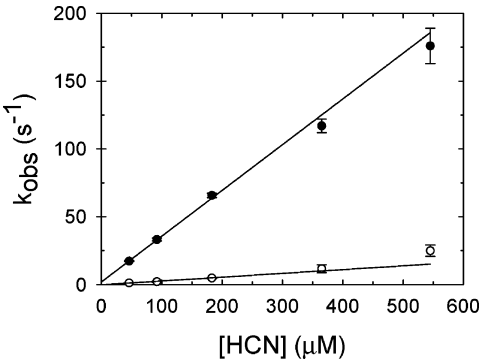

FIGURE 7: Plots of the observed rate constants for the reaction of HCN and CcP(H52K) as a function of the HCN concentration at pH 6.0 and 25 °C: (●) major phase of the reaction with an amplitude of ~80% of the absorbance change at 428 nm and (○) minor phase of the reaction. The solid lines are determined by weighted linear least-squares regression fitting of the data to eq 1 in the text. Apparent association rate constants for the fast and slow phases are $(3.4 \pm 0.1) \times 10^5$ and $(2.8 \pm 0.2) \times 10^4$ M^{-1} s^{-1}, respectively. Apparent dissociation rate constants (*Y*-intercepts) are 1.9 ± 0.5 and -0.2 ± 0.2 s^{-1} for the fast and slow phases, respectively.

Spectral properties of the CcP(H52K) cyanide complex at pH 6.0 are collected in Table 1.

Kinetics of Cyanide Binding. At pH 6.0, the binding of cyanide to CcP(H52K) is biphasic with each of the two observed rate constants linearly dependent upon the cyanide concentration (Figure 7). The amplitude of the slow reaction phase contributes ~20% to the total absorbance change at 428 nm. The observed pseudo-first-order rate constants were fit to eq 1 using weighted linear least-squares regression. The slopes of the two plots give the apparent association rate constant for HCN binding (k_{1a}) for the major component of CcP(H52K) and k_{2a} for the minor component. Best-fit values for k_{1a} and k_{2a} are $(3.4 \pm 0.1) \times 10^5$ and $(2.8 \pm 0.2) \times 10^4$ M^{-1} s^{-1}, respectively. The major component of CcP(H52K) reacts ~3 times more rapidly with HCN than does wild-type CcP at pH 6.0 (*12*).

The intercepts on the ordinate of Figure 7 give apparent dissociation rate constants for the major component (k_{1d}) and the minor component (k_{2d}). Best-fit values for k_{1d} and k_{2d} are 1.9 ± 0.5 and -0.2 ± 0.2 s^{-1}, respectively. Extrapolation of the observed rate constants to the ordinate gives intercepts very close to the origin, and the dissociation rate constants are not accurately determined by this method, although the near-zero intercepts confirm the very tight binding of cyanide.

Conformational States. The kinetic evidence indicates that there are at least three conformational states of CcP(H52K) that have differential reactivity toward both hydrogen peroxide and HCN. Two of these states are apparent from the kinetic data shown in Figures 4 and 7 with major (~80% of the reaction amplitude) and minor phases reacting independently with both hydrogen peroxide and HCN. These observations indicate that the two conformations do not interconvert on the time scale of the kinetic experiments (interconversion rates of <1 s^{-1}). Evidence for a third conformation comes from the 25% of the enzyme does not react with hydrogen peroxide and the long equilibration times required for binding of HCN to CcP.

Conclusions. Lys-52 can act as a base catalyst to accelerate the reactions of the mutant enzyme with both hydrogen peroxide and HCN. Although Lys-52 ($pK_a = 6.4$) is a stronger base than His-52 ($pK_a = 3.9$ in buffers not containing NO_3^-), the rate of the reaction with hydrogen peroxide is ~50-fold slower for the mutant enzyme, indicating that factors other than base strength limit the reaction. The association rate constants for binding of HCN to CcP(H52K) are nearly identical to the second-order rate constants for the reaction with hydrogen peroxide. The similarity in rates for HCN binding and Compound I formation for both the major and minor components of CcP(H52K) strongly suggests that the rate-limiting step in Compound I formation is binding of hydrogen peroxide to the heme iron and that HCN can act as a surrogate for hydrogen peroxide in its initial interaction with the heme iron in CcP and its mutants.

REFERENCES

1. Zamocky, M., Janecek, S., and Koller, F. (2000) Common phylogeny of catalase-peroxidases and ascorbate peroxidases, *Gene 256*, 169−182.
2. Poulos, T. L., Freer, S. T., Alden, R. A., Edwards, S. L., Skoglund, U., Takio, K., Eriksson, B., Xuong, N.-h., Yonetani, T., and Kraut, J. (1980) The crystal structure of cytochrome *c* peroxidase, *J. Biol. Chem. 255*, 575−580.
3. Finzel, B. C., Poulos, T. L., and Kraut, J. (1984) Crystal structure of yeast cytochrome *c* peroxidase refined at 1.7-Å resolution, *J. Biol. Chem. 259*, 13027−13036.
4. Poulos, T. L., and Kraut, J. (1980) The stereochemistry of peroxidase catalysis, *J. Biol. Chem. 255*, 8199−8205.
5. Erman, J. E., Vitello, L. B., Miller, M. A., Shaw, A., Brown, K. A., and Kraut, J. (1993) Histidine 52 is a critical residue for rapid formation of cytochrome *c* peroxidase compound I, *Biochemistry 32*, 9798−9806.
6. Miller, M. A., Shaw, A., and Kraut, J. (1994) 2.2-Å structure of oxy-peroxidase as a model for the transient enzyme:peroxide complex, *Nat. Struct. Biol. 1*, 524−531.
7. Poulos, T. L., and Finzel, B. (1984) Heme enzyme structure and function, *Pept. Protein Rev. 4*, 115−171.
8. Loo, S., and Erman, J. E. (1975) A kinetic study of the reaction between cytochrome *c* peroxidase and hydrogen peroxide: dependence on pH and ionic strength, *Biochemistry 14*, 3467−3470.
9. Palamakumbura, A. H., Foshay, M. C., Vitello, L. B., and Erman, J. E. (1999) Oxidation of cytochrome *c* peroxidase to compound I by peroxyacids: evidence for rate-limiting diffusion through the protein matrix, *Biochemistry 38*, 15647−15652.
10. Erman, J. E. (1974) Kinetic studies of fluoride binding by cytochrome *c* peroxidase, *Biochemistry 13*, 34−39.
11. Erman, J. E. (1974) Kinetic and equilibrium studies of cyanide binding by cytochrome *c* peroxidase, *Biochemistry 13*, 39−44.
12. Savenkova, M. I., Satterlee, J. D., Erman, J. E., Siems, W. F., and Helms, G. L. (2001) Expression, purification, characterization, and NMR studies of highly deuterated recombinant cytochrome *c* peroxidase, *Biochemistry 40*, 12123−12131.
13. Takio, K., Titani, K., Ericsson, L. H., and Yonetani, T. (1980) Primary structure of yeast cytochrome *c* peroxidase. II. The complete amino acid sequence, *Arch. Biochem. Biophys. 203*, 615−629.
14. Teske, J. G., Savenkova, M. I., Mauro, J. M., Erman, J. E., and Satterlee, J. D. (2000) Yeast cytochrome *c* peroxidase expression in *Escherichia coli* and rapid isolation of various highly purified holoenzymes, *Protein Expression Purif. 19*, 139−147.
15. Berry, E. A., and Trumpower, B. L. (1987) Simultaneous determination of hemes a, b, and c from pyridine hemochrome spectra, *Anal. Biochem. 161*, 1−15.
16. Kolthoff, I. M., and Belcher, R. (1957) *Volumetric Analysis*, Vol. 3, p 75, Interscience, New York.
17. Nelson, D. P., and Kiesow, L. A. (1972) Enthalpy of decomposition of hydrogen peroxide by catalase at 25 °C (with molar extinction coefficients of H_2O_2 solutions in the UV), *Anal. Biochem. 49*, 474−478.
18. Dhaliwal, B. K., and Erman, J. E. (1985) A kinetic study of the alkaline transitions in cytochrome *c* peroxidase, *Biochim. Biophys. Acta 827*, 174−182.
19. Vitello, L. B., Erman, J. E., Mauro, J. M., and Kraut, J. (1990) Characterization of the hydrogen peroxide-enzyme reaction for

two cytochrome *c* peroxidase mutants, *Biochim. Biophys. Acta 1038*, 90−97.
20. Hendler, R. W., and Shrager, R. I. (1994) Deconvolutions based on singular value decomposition and the pseudoinverse: a guide for beginners, *J. Biochem. Biophys. Methods 28*, 1−33.
21. Jordi, H. C. (1974) A kinetic study of the oxidation of ferrocyanide by compounds I and II of cytochrome *c* peroxidase, Ph.D. Dissertation, Northern Illinois University, DeKalb, IL.
22. Vitello, L. B., Erman, J. E., Miller, M. A., Mauro, J. M., and Kraut, J. (1992) Effect of Asp-235 → Asn substitution on the absorption spectrum and hydrogen peroxide reactivity of cytochrome *c* peroxidase, *Biochemistry 31*, 11524−11535.
23. Conroy, C. W., and Erman, J. E. (1978) Proton stoichiometry of the cytochrome *c* peroxidase mechanism as a function of pH, *Biochim. Biophys. Acta 527*, 370−378.
24. Lent, B., Conroy, C. E., and Erman, J. E. (1976) The effect of ionic strength on the kinetics of fluoride binding to cytochrome *c* peroxidase, *Arch. Biochem. Biophys. 177*, 56−61.
25. Gross, M. T., and Erman, J. E. (1985) Thermal denaturation of cytochrome *c* peroxidase: pH dependence, *Biochim. Biophys. Acta 830*, 140−146.
26. Conroy, C. W., Tyma, P., Daum, P. H., and Erman, J. E. (1978) Oxidation−reduction potential measurements of cytochrome *c* peroxidase and pH dependent spectral transitions in the ferrous enzyme, *Biochim. Biophys. Acta 537*, 62−69.
27. Miller, M. A., Coletta, M., Mauro, J. M., Putnam, L. D., Farnum, M. F., Kraut, J., and Traylor, T. G. (1990) CO recombination in cytochrome *c* peroxidase: effect of the local heme environment on CO binding explored through site-directed mutagenesis, *Biochemistry 29*, 1777−1791.
28. Erman, J. E., and Vitello, L. B. (1998) Cytochrome *c* peroxidase: a model heme protein, *J. Biochem. Mol. Biol. 31*, 307−327.
29. Erman, J. E., and Yonetani, T. (1975) A kinetic study of the endogenous reduction of the oxidized sites in the primary cytochrome *c* peroxidase-hydrogen peroxide compound, *Biochim. Biophys. Acta 393*, 350−357.
30. Erman, J. E., and Yonetani, T. (1975) The oxidation of cytochrome *c* peroxidase by hydrogen peroxide: characterization of products, *Biochim. Biophys. Acta 393*, 343−349.
31. Foshay, M. C. (2002) A study of structure/function relationships in cytochrome *c* peroxidase: base catalysis and hydrogen-bonding in the formation of compound I, Ph.D. Dissertation, Northern Illinois University, DeKalb, IL.

BI036240J